Flow Control of Vortical Structures and Vortex Breakdown Over Slender Delta Wings

Anthony Mitchell and Scott Morton
United States Air Force Academy, Department of Aeronautics
2354 Fairchild Drive, Suite 6F49
USAF Academy, CO 80840-6222, USA

Pascal Molton
Office National d'Etudes et de Recherches Aérospatiales (ONERA)
Fundamental and Experimental Aerodynamics Department
8 rue des Vertugadins, Meudon 92190, France

Yair Guy
Israeli Armament Development Authority, Israel

ABSTRACT

An understanding of the vortical structures and vortex breakdown is essential for the development of highly maneuverable and high angle of attack flight. This is primarily due to the physical limits these phenomena impose on aircraft and missiles at extreme flight conditions. In today's competitive world, demands for more maneuverable and stealthy air vehicles have encouraged the development of new control concepts for separated flows. The goal of this paper is to describe experimental flow control techniques used to manipulate the vortical structures and vortex breakdown over slender delta wings at high angles of attack.

The paper begins with a review of the experimental vortical flow control techniques implemented and tested over the past 50 years. This is by no means a comprehensive review, but is representative of the various flow control techniques examined. Beyond the brief historical review, this paper will examine more closely, two promising and different pneumatic flow control methods for the control of vortex breakdown over slender delta wings: open-loop, along-the-core blowing and periodic blowing and suction along the leading edges. These studies were performed at Onera and at the US Air Force Academy and consist of both experimental and computational analysis of subsonic flow fields around 70° delta wings over a broad range of angles of attack ($20° < \alpha < 40°$) and root-chord Reynolds numbers ($2x10^5 < Re_c < 2.6x10^6$).

INTRODUCTION

The delta wing flow field is dominated by vortical structures, the most prominent called leading-edge vortices. As angle of attack increases, these leading-edge vortices experience a sudden disorganization, known as vortex breakdown which can be described by a rapid deceleration of both the axial and swirl components of the mean velocity and, at the same time, a dramatic expansion of the vortex core. Henri Werlé first photographed the vortex breakdown phenomenon in 1954, during water tunnel tests of a slender delta wing model at Onera.[1] This work was quickly confirmed by Peckham and Atkinson,[2] Elle[3] and Lambourne and Bryer[4] and spawned a large number of experimental, computational and theoretical studies which continue today. These investigations led to the development of several theories governing vortex breakdown, although none have been universally accepted.[5-9] Despite this lack of a unified theoretical interpretation, several forms of vortex breakdown have been identified[7,10] and the global characteristics of the phenomena are understood. During the breakdown process, the mean axial velocity component rapidly decreases until it reaches a stagnation point and/or becomes negative on the vortex axis. This stagnation point, called the breakdown location, is unsteady and typically oscillates about some mean position along the axis of the vortex core[11,12] (see Fig. 1). As angle of attack is increased, the vortex breakdown location moves upstream over the delta wing (from the trailing edge toward the apex).

Werlé[13] was one of the first researchers to implement an active technique of controlling the vortical flow around a delta wing using either suction aft of the trailing edge or by injecting a mass flow over the delta wing. His original, qualitative study confirmed the capability of external methods to manipulate both the vortical structure and the vortex breakdown location. Additional flow control research initiated during the 1960's, at Onera[1415,16] and elsewhere[17-22] has led to a vast and varying

Paper presented at the RTO AVT Symposium on "Advanced Flow Management: Part A – Vortex Flows and High Angle of Attack for Military Vehicles", held in Loen, Norway, 7-11 May 2001, and published in RTO-MP-069(I).

Report Documentation Page

Form Approved
OMB No. 0704-0188

1. REPORT DATE	2. REPORT TYPE	3. DATES COVERED
00 MAR 2003	**N/A**	**-**

4. TITLE AND SUBTITLE	5a. CONTRACT NUMBER
Flow Control of Vortical Structures and Vortex Breakdown Over Slender Delta Wings	5b. GRANT NUMBER
	5c. PROGRAM ELEMENT NUMBER
6. AUTHOR(S)	5d. PROJECT NUMBER
	5e. TASK NUMBER
	5f. WORK UNIT NUMBER
7. PERFORMING ORGANIZATION NAME(S) AND ADDRESS(ES) **NATO Research and Technology Organisation BP 25, 7 Rue Ancelle, F-92201 Neuilly-Sue-Seine Cedex, France**	8. PERFORMING ORGANIZATION REPORT NUMBER
9. SPONSORING/MONITORING AGENCY NAME(S) AND ADDRESS(ES)	10. SPONSOR/MONITOR'S ACRONYM(S)
	11. SPONSOR/MONITOR'S REPORT NUMBER(S)

12. DISTRIBUTION/AVAILABILITY STATEMENT
Approved for public release, distribution unlimited

13. SUPPLEMENTARY NOTES
Also see: ADM001490, Presented at RTO Applied Vehicle Technology Panel (AVT) Symposium held inLeon, Norway on 7-11 May 2001, The original document contains color images.

14. ABSTRACT

15. SUBJECT TERMS

16. SECURITY CLASSIFICATION OF:			17. LIMITATION OF ABSTRACT	18. NUMBER OF PAGES	19a. NAME OF RESPONSIBLE PERSON
a. REPORT	b. ABSTRACT	c. THIS PAGE			
unclassified	**unclassified**	**unclassified**	**UU**	**14**	

Standard Form 298 (Rev. 8-98)
Prescribed by ANSI Std Z39-18

number of techniques to control the vortical flow structure around delta wings. It is not our intention to provide a detailed historical review of these previous works, but to represent the various techniques investigated.

Flow control methods for vortex dominated flows include both passive and active flow control using both mechanical and/or pneumatic systems to influence the vortical structures, vortex breakdown and other key characteristics which influence these phenomena. Mechanical techniques of vortical flow control include using canards, leading-edge extensions (LEX),[23] flaps[24,25] and strakes[26] as well as diverse combinations of these mechanical devices and other more exotic ideas such as variable sweep.[27] Pneumatic techniques consist of numerous blowing and suction configurations including: leading-edge injection,[28] along-the-core blowing,[29-33,12] spanwise blowing,[34,35] blowing parallel to the leading-edge,[36,37,38] tangential blowing around rounded leading edges,[39] trailing edge injection,[40-43] various applications of suction,[44,45] periodic blowing and suction[46-49] as well as other combinations of these pneumatic techniques. Many of the pneumatic techniques, whether open-loop or closed-loop, have been investigated experimentally by implementing external probes around the models or by installing internal systems within the models.

The remainder of this paper will give a detailed look at two promising pneumatic techniques to control vortex breakdown. Both techniques are applied to a 70^o delta wing and can be described as along the core blowing and periodic suction and blowing out of the leading edges. In addition to presenting two distinct pneumatic flow control methods, this paper also highlights two methods of non-intrusively diagnosing the flowfield, Laser Doppler Velocimetry and Computational Fluid Dynamics

Part I: Along the Core Blowing

This section describes the results of experiments conducted at Onera in the Fauga-Mauzac center's F2 subsonic, closed-return, atmospheric wind tunnel. The analysis described in this section primarily concerns the manipulation of the vortex breakdown location by along-the-core blowing.

EXPERIMENTAL FACILITIES

Onera's F2 wind tunnel has a rectangular test section with a width of 1.4m, a height of 1.8m, and a length of 5m. It is powered by a 680kW DC motor that drives a fan with blades spanning 3.15m and provides a maximum free-stream velocity in the test section of 105m/s. A cooling system in the closed-return portion of the wind tunnel facility maintains a constant free-stream temperature in the test section. The relative free-stream velocity, $\Delta U_0/U_0$, is estimated to have an accuracy of 1% while the mean intensity of turbulence has an accuracy of 0.1%.[50]

In F2, the delta wing model was mounted on a sting with a horizontal support and flexible joint for adjusting the angle of attack, with an accuracy of $\pm$ 0.05°. The horizontal support was manipulated in height along a vertical column so as to maintain the model close to the center axis of the test section. The model was mounted in the test section with no yaw angle with respect to the free-stream flow (estimated accuracy of $\pm$ 0.1°).

DELTA WING MODEL

Onera's sharp-edged, delta wing model has a 70° sweep angle (Λ) and root chord (c) of 950mm (Fig. 2). The model has a wingspan of 691.5mm at its trailing edge, is 20mm thick, and is beveled on the windward side at an angle of 15° to form a sharp leading edge. The delta wing is equipped with an internal system of tubing that provides regulated compressed air to two nozzles located near the apex, which are symmetrically situated about the root chord. The nozzles are located 14% of the root chord downstream of the apex of the wing and are situated 30mm from each leading edge. The position of a nozzle close to the leading edge, and near the apex was reported to be an optimal position for maximizing control and minimizing the blowing mass flow rate.[38] Each nozzle consists of a circular jet that expands from an interior diameter of 2.07mm into an open duct at an angle of 15.6° with respect to the leeward surface of the wing. The compressed air jet exits both nozzles slightly inward of the leading-edge vortex cores (5°) which corresponds closely to the optimal orientation presented by Guillot and al.[30] Sonic jet exit velocities (V_{jet}), based on isentropic relations and the measured total pressure of the compressed air, exist for all blowing mass flow rates considered in this study.

EXPERIMENTAL METHOD

This research is a continuation of earlier studies at Onera by Pagan[51], Laval-Jeantet[52] who examined open-loop, along-the-core blowing as an effective method of controlling the breakdown location. The objective of this study is to examine the influence of along-the-core blowing to eliminate or delay the vortex breakdown location. A detailed analysis of the principle

characteristics of the phenomena, with and without flow control, is presented based on Laser Doppler Velocimetry (LDV) measurements. The results provide details on the physical properties of the vortical structures which are altered by along-the-core blowing and the resulting influence on the vortex breakdown location. All of the data presented here was acquired at test conditions of U_∞ = 24m/s ($Re_c = 1.56x10^6$) and $\alpha = 27°$. Along-the-core blowing mass flow rates were varied, symmetrically and asymmetrically, to compare their influence on the breakdown location of each vortex, controlled and uncontrolled. Blowing mass flow rates of 1.4, 1.8, 2 and 2.2g/s for each nozzle were studied, corresponding to blowing momentum coefficients (C_μ) of 0.004, 0.005, 0.0057, 0.006.

Laser Doppler Velocimetry

The 3-D LDV system at Onera, installed around the test section in F2, utilizes two 15W argon lasers as the sources of light in both the forward and backward scattering mode. The forward scattering mode provides a higher signal to noise ratio than a backward scattering mode, but is not always available due to the position of the model in the test section and the desired measurement grid. Smoke particles from incense or theater smoke machines are emitted into the wind tunnel downstream of the test section so as to avoid disturbing the flow field in the test section.

For each volume of exploration, the three instantaneous velocity components related to a specific particle are acquired. Using statistical methods, the mean velocity component in each of the three directions as well as the Reynolds tensors are then calculated from a total of 2000 particles. Unfortunately, the acquisition time of these 2000 particles varies with respect to the measurement volume's position in the flow field due to the non-uniform density of the seeding particles in the separated vortical structures. The global accuracy of the LDV system is estimated to have a relative error, $\Delta U/U$, of less than 1.5% assuming an absolute error of the angle between the velocity vector and a horizontal reference of 0.5°. The measurements were repeatable and angles were always smaller than the estimated error assumption, thus leading to an estimated accuracy of the magnitude of the velocity to ± 1m/s and of the direction of the velocity vector to ± 1°.[53]

ALONG-THE-CORE BLOWING RESULTS

Fig. 3 presents the non-dimensional mean axial velocity component (U/U_∞) in the longitudinal plane intersecting the leading-edge vortex cores without blowing (Fig. 3a) and for three different asymmetric blowing mass flow rates (Figs. 3b, 3c and 3d). In these cases, the asymmetric blowing is along the portside of the model. Previous studies have shown the independence of asymmetric and symmetric blowing on the influence of the vortex breakdown location.[31,32] The gray background represents the leeward surface of the wing with the leading edge being denoted by the border between the white and gray background. For all configurations, a strong, jet-like, acceleration of the flow along the vortex core is observed upstream of vortex breakdown with maximum values of $U/U_\infty \geq 3.8$.

In Fig. 3 one also observes an abrupt deceleration of the axial velocity component to a stagnation point (vortex breakdown location) that is followed by a zone of recirculation and a sizeable increase in the diameter of the vortex core. The post breakdown region has a wake-like axial velocity profile. The mean portside breakdown location without blowing was identified at $X_b/c = 0.65$. For a Q_m = 1.4g/s, the mean breakdown location was displaced aft approximately 8% of the chord to $X_b/c = 0.73$. As the blowing mass flow rate was increased to Q_m = 1.8g/s, the mean breakdown location was shifted downstream 13%c to $X_b/c = 0.78$. Finally for Q_m = 2.2g/s, the mean breakdown location is shifted downstream to a location aft of the measurement plane ($X_b/c = 0.95$).

These results confirm laser sheet visualization results that have demonstrated the dependence of the control of the vortex breakdown location on the blowing mass flow rate. In Fig. 3, it is clear that as the blowing mass flow rate increases, the vortex breakdown location is shifted further downstream toward the trailing edge. Except for the downstream displacement of the mean vortex breakdown location, the vortical structure and recirculation region do not appear to change as a result of the along-the-core blowing. For all of these blowing configurations, a strong, jet-like, acceleration of the flow along the vortex core is observed upstream of vortex breakdown location. The breakdown phenomenon includes an abrupt deceleration of the axial velocity component to a stagnation point that is followed by a recirculation zone and a sizeable increase in the diameter of the vortex core. The post breakdown region maintains its wake-like axial velocity profile. Unfortunately, in Fig. 3, it is difficult to assess the mechanisms through which the along-the-core blowing manipulates the leading-edge vortex and its breakdown location. Therefore, an analysis of the influence of the various blowing mass flow rates on the velocity profiles upstream of the vortex breakdown locations is necessary.

In Fig. 4,axial (U/U_∞) and tangential (W/U_∞) velocity components are traced from data acquired at 2 fixed chordwise locations ($X/c = 0.53$ and 0.63) for three blowing mass flow rates as well as the reference configuration without blowing. Although the

blowing mass flow rate is increased systematically from 0 to 2.2g/s, there is no significant modification of the three parameters shown in these plots.

Another method of analyzing the influence of the flow control on the breakdown location is needed. The LDV measurements in perpendicular planes located 0.02c upstream of each stagnation point for the respective blowing mass flow rates are plotted in Fig. 5. Obviously, as the blowing mass flow rate is increased and the breakdown location is shifted downstream, the measurement plane must also be adjusted. In Fig. 5, the data are acquired in planes situated at: X/c = 0.63 without blowing; X/c = 0.72 for a Q_m = 1.4g/s; and X/c = 0.76 for a Q_m = 1.8g/s. The corresponding axial and tangential velocity components are regrouped and the data silhouette identical curves. The characteristics of the vortical structures at fixed locations upstream of vortex breakdown are identical for the reference configuration and for blowing mass flow rates of 1.4g/s and 1.8g/s.

From these results, we conclude that along-the-core blowing does not modify the vortical structure upstream of the vortex breakdown location. The blowing simply increases the momentum in the vortex core that allows it to overcome the adverse pressure gradient generated by the trailing edge and shifts the vortex breakdown location downstream.

ALONG-THE-CORE BLOWING CONCLUSIONS

Open-loop blowing along each of the leading-edge vortices on the leeward surface of the delta wing was examined as a flow control technique to manipulate the vortex breakdown location. The LDV results confirm previous studies of the trends in the leading-edge vortices including the shift from a jet-like axial velocity profile upstream of the breakdown location to a wake-like profile. They are also used to identify the mechanism of the along-the-core blowing manipulation the vortex breakdown location. Both asymmetric and symmetric flow control configurations demonstrated the ability to displace the vortex breakdown location downstream toward the trailing edge of the delta wing. The ability of the various blowing configurations to manipulate the controlled breakdown location was dependent on the blowing mass flow rate and the freestream velocity. As the blowing mass flow rates increased, the effectiveness of the flow control improved and was more capable of delaying the vortex breakdown. Therefore, we conclude that along-the-core blowing simply increases the momentum in the vortex core and allows it to overcome the adverse pressure gradient generated by the trailing edge and shifts the vortex breakdown location downstream. The addition of momentum to the vortex core by along-the-core blowing is effective; however, it requires large amounts of energy to influence the breakdown location.

Part II: PERIODIC BLOWING AND SUCTION

The next pneumatic flow control technique is periodic suction and blowing from a slot along the leading-edge of a delta wing (Fig. 6). This section describes the results of the computational simulations, as well as comparison of these results with experiments obtained in the USAFA water tunnel. The analysis described in this section primarily concerns lateral and vertical motion of the vortex core and the breakdown location. Details of the water tunnel experiments can be found in References 46, 47, 54 and 55.

NUMERICAL METHOD

In this section a brief description of the numerical method is provided. Full details of the computational scheme and the solution method are presented in Refences 48 and 56. The flow field was computed over a flat-plate, semi-span delta wing with a leading-edge sweep of 70^o and a 25^o bevel on the lower surface. The wing had a root chord of 0.74m and a 3mm wide leading-edge slot extending the entire length. Solutions were obtained at an angle of attack $\alpha=35^o$, with and without periodic blowing and suction through the leading-edge slot. Blowing and suction was applied normal to the leading edge and parallel to the upper surface of the wing. The free stream velocity was 40m/s and the corresponding root-chord Reynolds number was 200,000. Periodic blowing and suction was applied at a nondimensional frequency of $F^+=2.2$ and the momentum coefficient was $C_\mu=0.007$.

Solutions were computed with the May 1999 version of the computer code $Cobalt_{60}$, developed by the Computational Sciences Branch at the Air Force Research Lab, AFRL/VAAC. $Cobalt_{60}$ solves the unsteady, three-dimensional, compressible Navier-Stokes equations on an unstructured grid. All runs were conducted with the laminar flow option of the code. A much more descriptive discussion of $Cobalt_{60}$ may be found in reference 56.

Boundary Conditions

At the forward boundary of the delta wing domain, Riemann invariant conditions are used to specify values of the dependent flow variables. Along the centerline of the configuration, a slip surface imposes symmetry, and Riemann invariant conditions are employed at the upper (outflow), lower (inflow), out-board lateral (outflow), and downstream (outflow) boundaries. On solid surfaces, the no slip conditions were enforced by adjusting the velocity dyad in cells adjacent to no-slip walls to ensure zero relative velocity over the entire wall face. The normal momentum equation is used at solid walls to estimate the variation of pressure normal to the wall, while the one-sided, least-squares gradient method is used to estimate the variation of pressure tangential to the wall.

The leading-edge slot is modeled with a normal velocity component that sinusoidally varies with time. There are two parameters that specify the periodic suction/blowing characteristics, $F^+ = (fC)/U_o$ and $C_\mu = 2(H/C)(\langle v' \rangle / U_o)^2$, where f is the dimensional frequency of oscillation, C is the delta wing chord, Uo is the freestream velocity, H/C is the ratio of slot width to delta wing chord, and <v'> is the RMS value of the sinusoidally varying slot normal velocity. With a known F^+, the frequency of oscillation is specified and with a known C_μ, the maximum normal velocity component is specified. The normal component of velocity out of the slot is resolved into the body axis system velocity components, u and v. The normal component to the delta wing surface, w, is specified to be zero. The velocities are assumed to be constant across the slot and down the length of the slot. The density is assumed to be constant at freestream, based on the low Mach number of the computations, and the normal momentum equation provides a condition for the pressure, p.

Computational Meshes

In the current research, unstructured grids suitable for viscous flows were developed by using two software packages: GridTool[57] and VGRIDns[58]. Initially, a 200,00 cell unstructured grid was developed but found to be inadequate to capture the small structures associated with vortex breakdown. The grid used for all runs in the current work, denoted the medium grid, had 138,000 points forming 591,000 cells. There were 10 layers of prism cells near the delta wing surface and the remaining cells in the volume were tetrahedrons. Solutions were also computed on a more refined grid with 285,326 points forming 1,235,091 cells to verify the accuracy of solutions on the medium grid. The average y^+ at the surface was approximately 1 for both the medium and fine grids. Solutions computed with the medium grid were in reasonable agreement with solutions on the fine grid allowing the medium grid to be used for the remainder of the study.

Time Step Sensitivity Studies

Extensive time-step, Newton-subiterate and numerical damping studies were completed and presented in Ref. 48. In these studies it was determined that time accuracy was achieved with a time step of 0.0001 seconds, 3 Newton-subiterates and a $Cobalt_{60}$ damping coefficient of 0.6 when using the second-order accurate time-integration option. The resulting time step required 86 time steps per period of oscillation and a period of oscillation required 28 minutes of run time on a 32 processor IBM SP3.

PERIODIC SUCTION/BLOWING RESULTS

Spatial and Temporal Location of The Vortex Core

Before the onset of vortex breakdown, the trajectory of the leading-edge vortex is straight[59]. The time-dependent spatial location of the vortex core was determined as the locus of all points having maximum vorticity, and the results are presented in Figs. 7, 8, and 9. The lateral location of the vortex core (see Fig. 1), with and without flow excitation, is plotted with respect to time in Fig. 7. The time is rendered nondimensional by the period of the periodic flow excitation, namely T=0.0086 sec and results are plotted over one cycle. The mean lateral location of the vortex core, without flow excitation, is $Y_c(nb)/b=0.668$ and its standard deviation is 0.015. This computed value is in good agreement with experimental values of $Y_c/b=0.6$[46] and $Y_c/b=0.65$[60], and with another computed value of $Y_c/b=0.65$[61]. With the periodic flow excitation on, the vortex core moves slightly inboard to a mean location of $Y_c(b)/b=0.654$, and the standard deviation increases to 0.081, much larger than without the flow excitation Fig. 7 also shows that the lateral movement of the vortex core has the same frequency as the flow excitation, and both are in-phase. The vortex moves outboard during the blowing phase, and moves inboard during the suction phase. Its maximum outboard location is at $Y_c(b)/b=0.67$, and coincides with the time of maximum blowing velocity at t/T=0.25. The maximum inboard location is at $Y_c(b)/b=0.53$, and coincides with the time of maximum suction velocity at t/T=0.75. At t/T=0 and t/T=1.0 (where the flow excitation vanishes), the lateral location of the vortex core coincides approximately with its location without flow excitation.

The vertical location of the vortex core is presented in Fig. 8, where the core angle relative to the wing (see Fig.1) is plotted with respect to the nondimensional time. Without flow excitation, the vortex-core angle relative to the wing fluctuates between α_c=6.7º and α_c=7.7º, around a mean value of α_c=7.3º. The mean angle is in very good agreement with another computed result[61] of α_c=7.5º, and in fair agreement with an experimental value of α_c=9.1º, measured by Guy *et al*[47] in a water-tunnel. With the periodic flow excitation activated, the fluctuations of the core angle increase significantly to a range of α_c=4.8º to α_c=9.3º, but the mean value of α_c=6.9º is only slightly lower than without flow excitation. Fig. 8 also shows that the frequency of the vertical movement of the vortex core is the same as the frequency of flow excitation, but there is a phase-shift of approximately 0.25T between the two.

The orbital movement of the vortex core is presented in Fig. 9, where the vertical location is plotted with respect to the lateral location, with and without flow excitation. The vortex-core movement without flow excitation seems to be erratic, and the fluctuations may represent a combination of natural fluctuations with data-reduction inaccuracies. When the flow excitation is activated, the vortex core follows an elliptical path, and its movement is clearly governed by the period and direction of the flow excitation.

Location of Vortex Breakdown

The breakdown point of the primary vortex is defined where the axial flow within the longitudinal vortex stagnates.[48] Some representative plots of the velocity distribution along the vortex core, with and without flow excitation, are presented in Figs. 10 and 11. Without flow excitation, the temporal velocity variations along the vortex core were found to be small, so for this case, only one plot is presented in Fig. 9. Vortex breakdown is identified at an axial location of X_b/C=0.4, in excellent agreement with the value X_b/C=0.4 established by Guy et al[47] in water-tunnel experiments, and well within the range $0.35<X_b/C<0.45$ that was compiled from numerous experiments.[59]

With flow excitation, the temporal velocity variations along the vortex core were found to be large, as were the fluctuations of the breakdown location. Two examples of the velocity distribution with flow excitation, during the blowing phase, are presented in Fig.10, for t/T=0.25 (maximum blowing velocity) and t/T=0.5 (zero blowing velocity). Vortex breakdown is clearly identified, its location varies between X_b/C=0.55 and X_b/C=0.65. These results indicate that vortex breakdown is delayed by 0.15 to 0.25 chordlengths, in good agreement with the value of 0.2 chordlengths found by Guy et al in wind tunnel experiments[46], and 0.33 chordlengths found in water tunnel experiments.[47]Duing the suction phase, the velocity in the vortex core is always positive (Fig.11), and vortex breakdown can not be identified.

Surface Pressure Distribution

The pressure distribution on the lower surface of the wing was computed and representative results at a chordwise location of X/C=0.3 are presented in Fig. 12. Without flow excitation, the pressure distribution does not vary with time, so for this case, only one plot is presented in Fig. 12. With flow excitation, the pressure on the lower surface varies at a frequency that corresponds to the frequency of the excitation. The pressure increases during the blowing phase and peaks at t/T=0.25, corresponding to the maximum blowing velocity. It decreases during the suction phase and reaches its lowest value at t/T=0.75, corresponding to the maximum suction velocity.

Overall, it seems that the pressure with flow excitation fluctuates around a mean value that is approximately equal to the pressure without flow excitation. Therefore, it may be expected that the pressure on the upper surface only will govern the effect of the flow excitation on the global characteristics of the wing. The pressure distribution on the upper surface of the wing was computed and representative results at chordwise locations of X/C=0.3, 0.5, and 0.7 are presented in Figs. 13, 14, and 15, respectively.

The pressure distribution at a chordwise location of X/C=0.3 is presented in Fig. 13. This location is ahead of the vortex breakdown with and without flow excitation (see Fig. 10), and the peak suction is high in all cases, as expected. The flow excitation has only a small effect on the pressure distribution, mainly over the outer part of the wing. The absolute value of the pressure coefficient increases during the blowing phase, and decreases during the suction phase, the mean being almost the same as without excitation. This indicates that the flow excitation does not affect the lift of this cross-section, as was also shown by Guy et al in wind tunnel and water tunnel experiments.[46,47,54,55]

It is worth noting that the peak suction appears at Y/b=0.67 (no excitation), Y/b=0.72 (excitation at maximum blowing, t/T=0.25), and Y/b=0.5 (excitation at maximum suction, t/T=0.75). These values match the spanwise locations of the vortex core at the corresponding instances (see Figs. 7 and 9), indicating that these points are right underneath the vortex core, where the tangential velocity is maximum.

The pressure distribution at a chordwise location of X/C=0.5 is presented in Fig. 14. This location is aft of the vortex breakdown-point without flow excitation, but ahead of the vortex breakdown-point with flow excitation (see Fig. 10). The peak pressure coefficient without flow excitation is $-C_p$=1.2, much lower than $-C_p$=2.6 at X/C=0.3 (see Fig. 13), clearly indicating vortex breakdown. The profound effect of the flow excitation is evident. At maximum blowing, the peak pressure coefficient is $-C_p$=2.4, much higher than without excitation. At maximum suction, the peak pressure coefficient is only slightly lower than without flow excitation. These values indicate that the contribution of the cross-section to the lift is greatly increased by the flow excitation. The pressure distribution at a chordwise location of X/C=0.7, aft of the breakdown with or without flow excitation, is presented in Fig. 15. The peak pressure coefficients are low in all cases, but the positive effect of the flow excitation in increasing the pressure coefficient is still evident.

The Normal Force

The pressure distribution over the upper and lower surface of the wing was integrated, to yield the normal force coefficient. The results are presented in Figs. 16 and 17.

The effect of the periodic flow excitation on the normal force is presented in Fig. 16, where the normal force coefficient is plotted with respect to the nondimensional time. Clearly, the flow excitation greatly increases the force, during the blowing phase as well as during the suction phase. The normal force varies with time, but there is no clear indication that the period of this variation corresponds to the period of the flow excitation.

The ratio of the normal force coefficients, with and without flow excitation, is presented in Fig. 17. Some fluctuations are observed, but they do not seem to correspond to the period of the flow excitation. The periodic flow excitation increases the normal force by 24% to 30%, in very good agreement with an increase of 25% found by Guy et al[54] in wind tunnel experiments.

Vortex Core Motion Visualization

Iso-surfaces of entropy were computed, to better visualize the location of the vortex-core. Top views of the wing and the computed iso-surfaces are presented in Fig. 18 (no flow excitation), Fig. 20 (flow excitation at maximum blowing), and Fig. 22 (flow excitation at maximum suction). These images can be compared with images of the vortex core obtained in water-tunnel experiments,[47,54] presented in Figs 19, 21 and 23, at the corresponding instances. The computed vortex locations are in very good agreement with the experimental results. Table 1 below summarizes the comparison in terms of the lateral position of the vortex core.

PERIODIC SUCTION/BLOWING CONCLUSIONS

A critical examination of the results obtained from a numerical simulation of the flow field on a delta wing with periodic blowing and suction was presented. The results indicate that the computational scheme properly captured the effect of periodic blowing and suction on the main parameters of the flowfield and on the normal force of the wing. The periodic flow excitation induces vortex movement in both lateral and vertical directions. As a result, the vortex core follows an elliptical path, at a frequency that corresponds to the frequency of the flow excitation. The periodic flow excitation delays vortex breakdown by over 0.25 chordlengths and increases the normal force of the wing by approximately 27%. All of these results are in very good agreement with previously obtained experimental results.

CONCLUDING REMARKS

Both flow control techniques, along-the-core blowing and periodic suction and blowing along the leading-edges, have been shown to manipulate the vortex breakdown location over slender delta wings at high angles of attack. Each technique provides unique advantages for the control of the vortex breakdown location depending on the desired outcome.

Along-the-core blowing demonstrated the ability to control the breakdown location as a function of the blowing mass flow rate and the freestream velocity. Increased blowing mass flow rates augmented the momentum in the vortex core which delayed breakdown by overcoming the adverse pressure gradient generated by the trailing edge. The addition of momentum to the vortex core by along-the-core blowing is effective; however, it requires large amounts of energy to influence the breakdown location.

Periodic suction and blowing induced vortex movement in both lateral and vertical directions. The periodic flow excitation delayed vortex breakdown by over 0.25 chordlengths and increases the normal force of the wing by approximately 27%. The delay of the vortex breakdown was accomplished with zero net mass.

In addition to presenting these two distinct pneumatic flow control methods, this paper has demonstrated the applicability of two powerful, non-intrusive diagnostic tools (Laser Doppler Velocimetry and Computational Fluid Dynamics) for evaluating and further understanding the complicated 3-D flowfield.

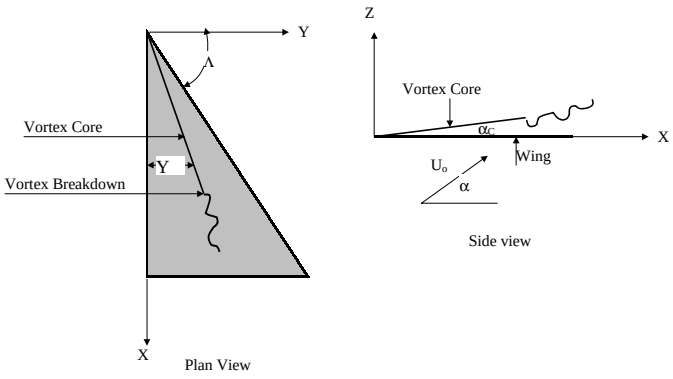

Fig. 1: Definition of the spatial location of the vortex core and the vortex breakdown location.

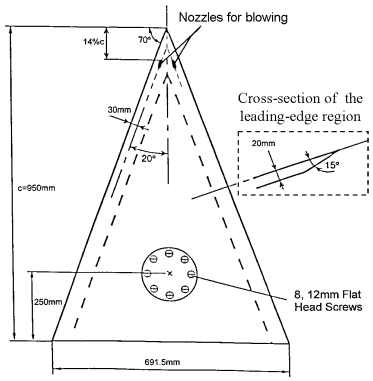

Fig. 2: Sketch of the delta wing model with nozzles for along-the-core blowing near the apex.

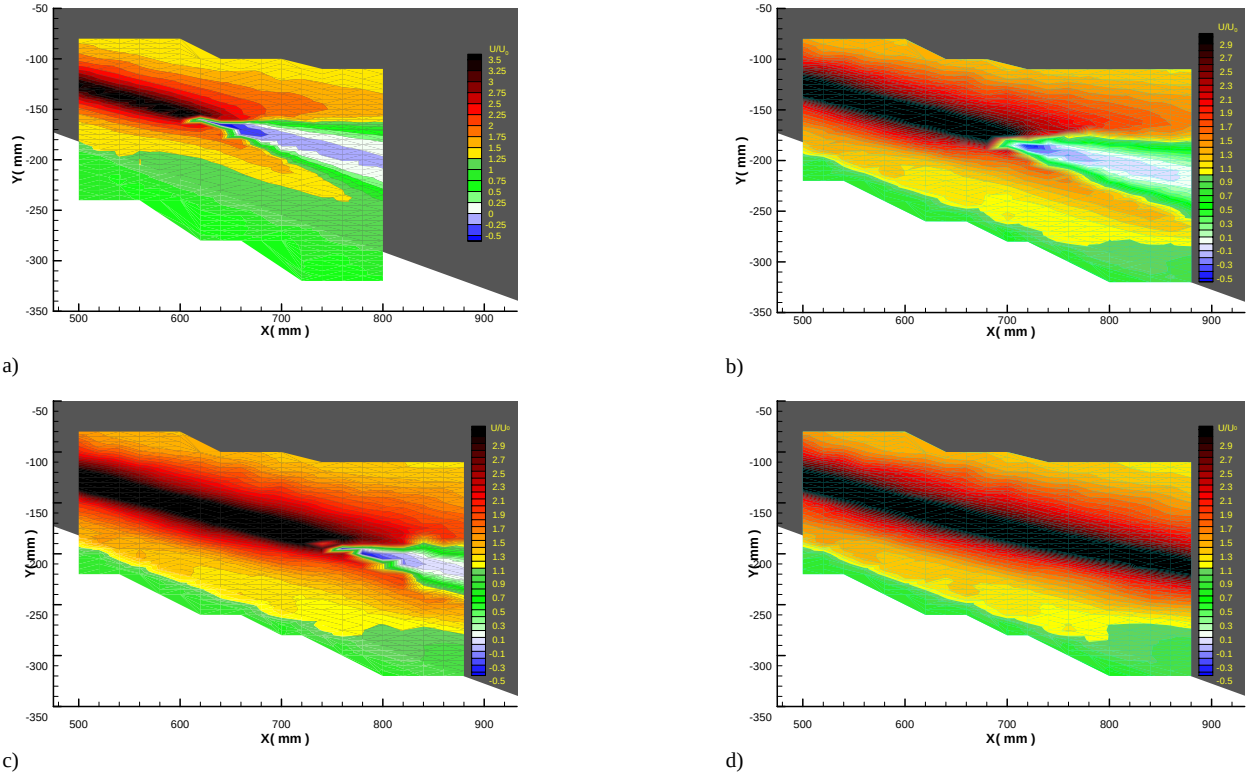

a) b)

c) d)

Fig. 3: LDV results of U/U_∞ in the longitudinal plane at $\alpha = 27^o$ and $U_\infty = 24$m/s. Portside along-the-core blowing with Q_m = (a) 0 (b)1.4g/s. (c) 1.8g/s (d) 2.2g/s.

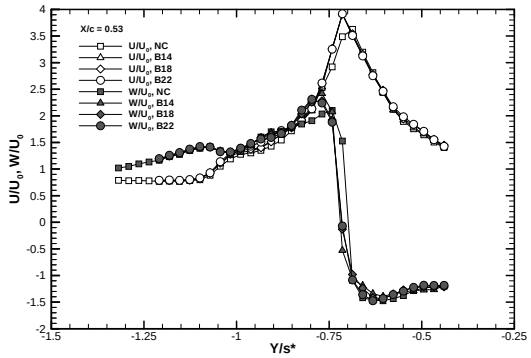

a)

b)

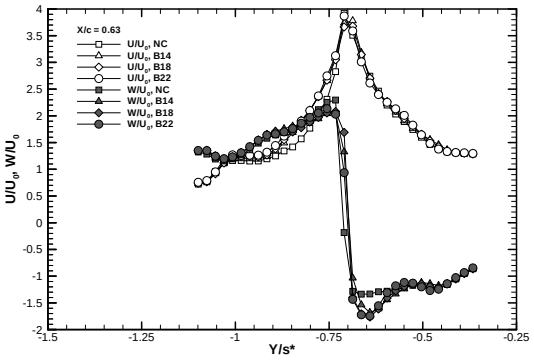

Fig. 4: U/U_∞ and W/U_∞ profiles at Q_m = 0, 1.4g/s, 1.8g/s and 2.2g/s (NC, B14, B18 and B22). Profile locations of (a) X/c=0.53 (b) X/c = 0.63.

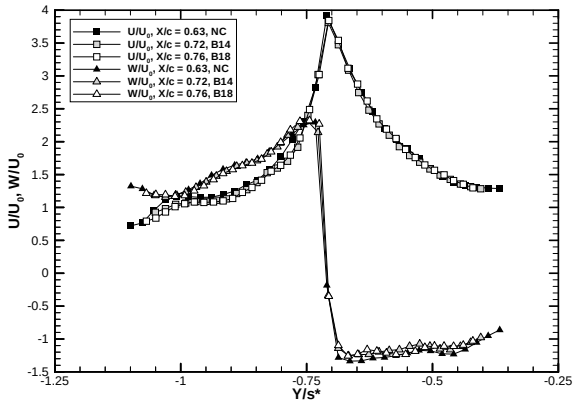

Fig. 5: U/U_∞ and W/U_∞ profiles upstream of the vortex breakdown location with no control (NC) and for two blowing mass flow rates Q_m = 1.4g/s and 1.8g/s (B14 and B18). Profiles at X/c = 0.63, 0.72 and 0.76.

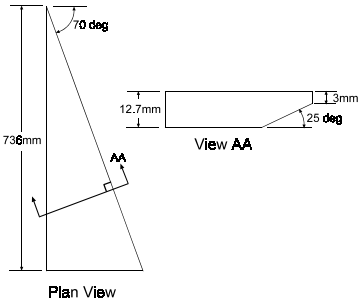

Fig. 6: Sketch of the delta wing model with periodic suction and blowing slot at the leading edge.

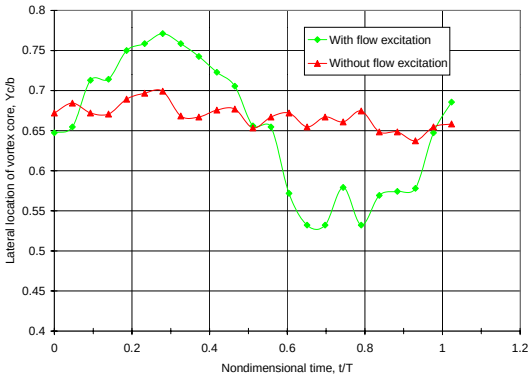

Fig. 7: Lateral movement of the vortex core.

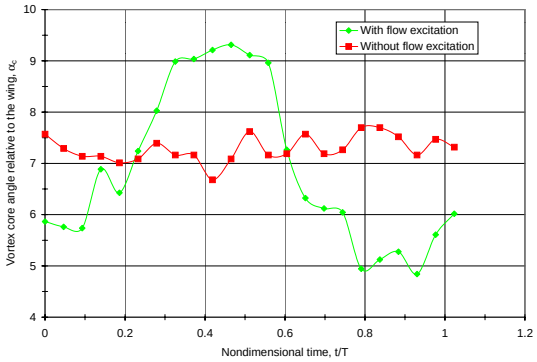

Fig. 8: Vortex-core angle relative to the wing.

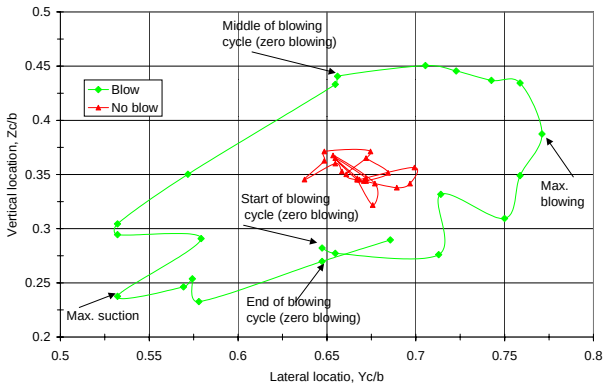

Fig. 9: Orbital movement of the vortex core.

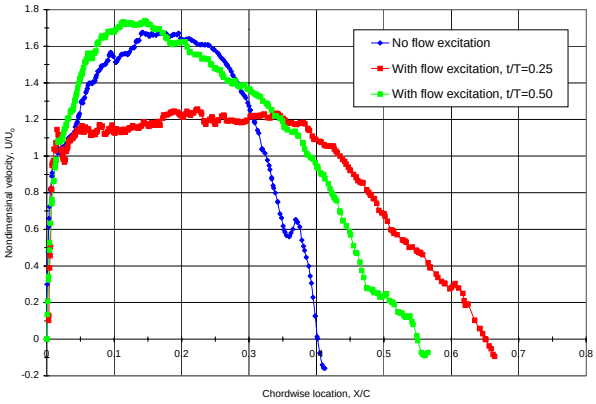

Fig. 10: Velocity distribution along vortex core, without flow excitation and during the blowing phase of flow excitation.

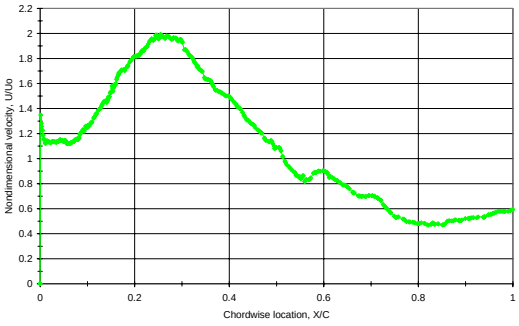

Fig. 11: Velocity distribution along vortex core, suction phase, flow excitation at maximum suction, t/T=0.75.

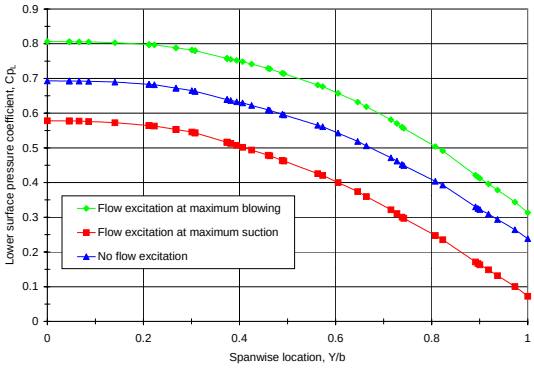

Fig. 12: Pressure distribution on the lower surface of the wing. Sample results at X/C=0.3.

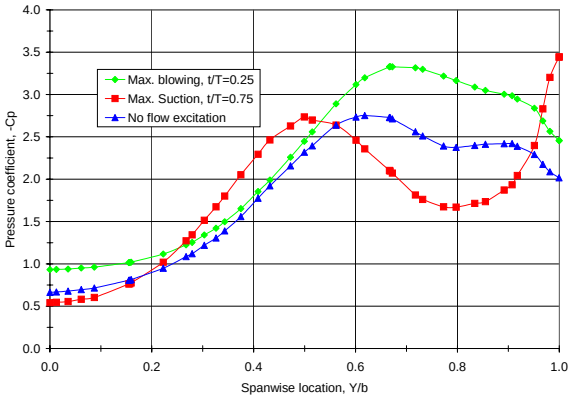

Fig. 13: Pressure distribution on the upper surface of the wing, chordwise location X/C=0.3.

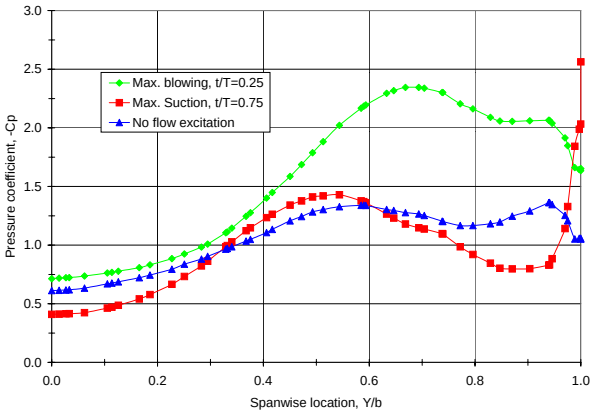

Fig. 14: Pressure distribution on the upper surface of the wing, chordwise location X/C=0.5.

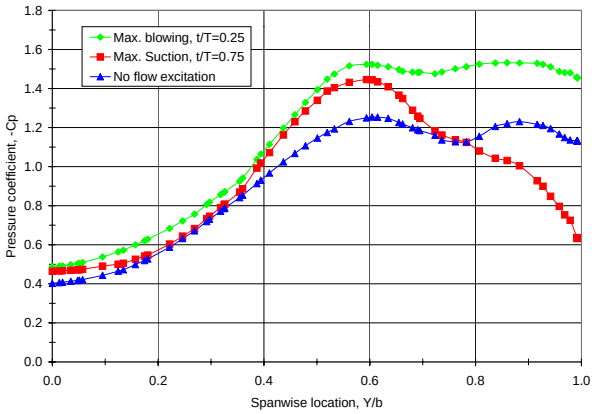

Fig. 15: Pressure distribution on the upper surface of the wing, chordwise location X/C=0.7.

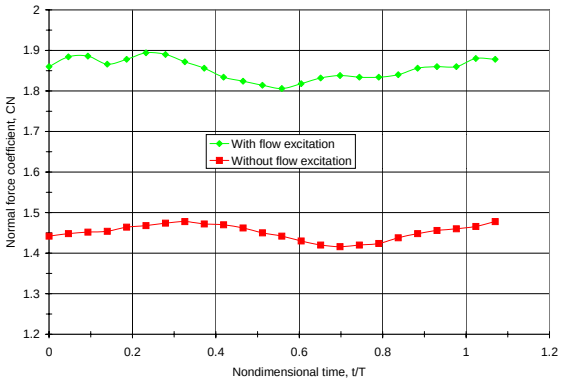

Fig. 16: Normal force coefficient.

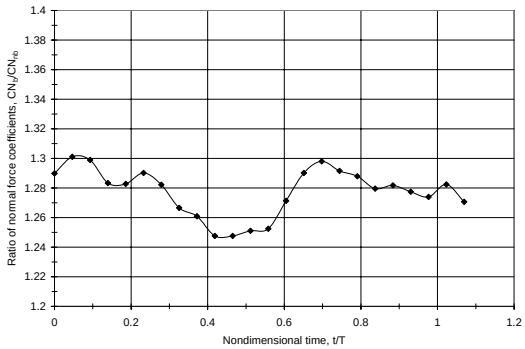

Fig. 17: Ratio of the normal force coefficient, with and without periodic flow excitation.

	No Excitation	Maximum Blowing	Maximum Suction
Computation Y_c/b	0.67	0.70	0.55
Experiment Y_c/b	0.67	0.74	0.54

Table 1: Comparison of computational and experimental results.

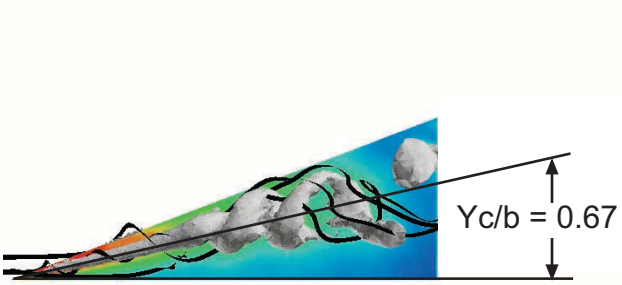

Fig. 18: Instantaneous contours of surface pressure and an iso-surface of entropy in the vortex core without suction/blowing, Y_c/b=0.67. (α=35°, Re=200,000)

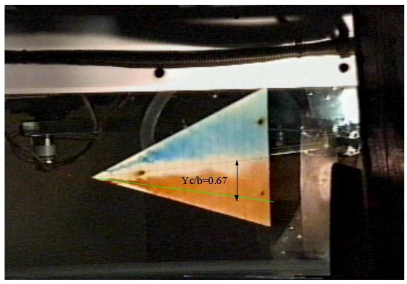

Fig. 19: Water Tunnel experiment without suction/blowing, Y_c/b=0.67. (α=35°, Re=33,000)

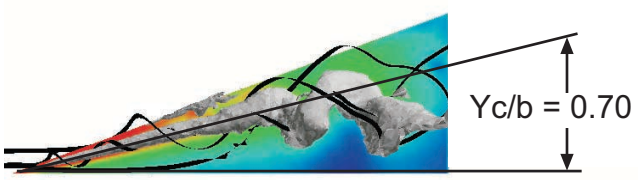

Fig. 20: Instantaneous contours of surface pressure and an iso-surface of entropy in the vortex core at maximum blowing, Y_c/b=0.70. (α=35°, Re=200,000)

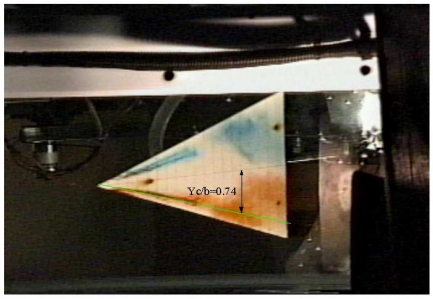

Fig. 21: Water Tunnel experiment at maximum blowing, Y_c/b=0.74. (α=35°, Re=33,000)

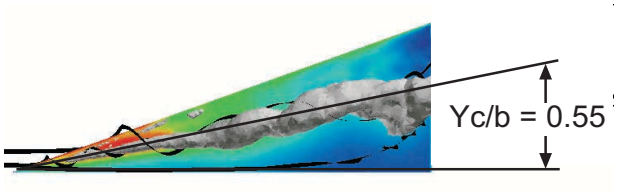

Fig. 22: Instantaneous contours of surface pressure and an iso-surface of entropy in the vortex core at maximum suction, $Y_c/b=0.55$. ($\alpha=35^o$, Re=200,000)

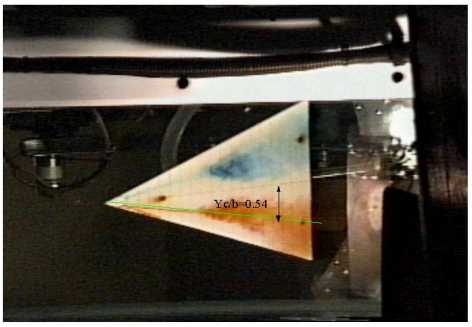

Fig. 23: Water Tunnel experiment at maximum suction, $Y_c/b=0.54$. ($\alpha=35^o$, Re=33,000)

[1] Werlé, H., "Quelques résultats expérimentaux sur les ailes en flèche, aux faibles vitesses, obtenus en tunnel hydrodynamique" *La Recherche Aéronautique*, No. 41, Sep.-Oct. 1954, pp. 15-21.

[2] Peckham, D.H., Atkinson, S.A., "Preliminary Results of Low Speed Wind Tunnel Tests on a Gothic Wing of Aspect Ration 1.0", Aeronautical Research Council Technical Report, C.P. No 508, T.N. Aero 2504, Apr. 1957.

[3] Elle, B.J., "An Investigation at Low Speed of the Flow near the Apex of Thin Delta Wings with Sharp Leading Edges", Aeronautical Research Council R&M, No. 3176, 1961.

[4] Lambourne, N.C., Bryer, D.W., "The Bursting of Leading-Edge Vortices-Some Observations and Discussion of the Phenomenon", Aeronautical Research Council R&M No. 3282, 1962.

[5] Hall, M.G., "Vortex Breakdown", *Annual Review of Fluid Mechanics*, Vol. 4, 1972, pp. 195-218.

[6] Leibovich, S., "The Structure of Vortex Breakdown," *Annual Review of Fluid Mechanics*, Vol. 10, 1978, pp. 221-46.

[7] Sarpkaya, T. "On Stationary and Traveling Vortex Breakdowns," *Journal of Fluid Mechanics*, Vol. 45, Part 3, 1971, pp. 545-559.

[8] Nelson, R.C., "Unsteady Aerodynamics of Slender Wings," Aircraft Dynamics at High Angles of Attack: Experiments and Modeling, AGARD-R-776, 1991, pp.1-1 to 1-26.

[9] Délery, J., "Aspects of Vortex Breakdown," *Progress in Aerospace Sciences*, Vol. 30, 1994, pp. 1-59.

[10] Faller, J.H., Leibovich, S., "Disrupted states of vortex flow and vortex breakdown", *Physics of Fluids*, Vol. 20, No. 9, 1977, pp.1385-1400.

[11] Menke, M., Yang, H., Gursul, I., "Further Experiments on Fluctuations of Vortex Breakdown Location," AIAA-96-0205, 34th AIAA Aerospace Sciences Meeting and Exhibit, Jan 1996, Reno, NV.

[12] Mitchell, A.M., Molton, P., Barberis, D., Délery, J., "Oscillation of Vortex Breakdown Location and Control of the Time-Averaged Location by Blowing", *AIAA Journal*, Vl. 38, No. 5, May 2000, pp.793-803.

[13] Werlé, H., "Sur l'éclatement des tourbillons d'apex d'une aile delta aux faibles vitesses", *La Recherche Aéronautique*, No 74, 1960.

[14] Werlé, H., Fiant, C., "Visualisation hydrodynamique de l'écoulement à base vitesse autour d'une maquette d'avion du type 'Concorde'," *La Recherche Aérospatiale*, No. 102, 1964.

[15] Poisson-Quinton, Ph., "Contrôle du décollement d'une surface portante par un jet transversal', ICAS paper, 7th Congress of the International Council of the Aeronautical Sciences, Rome, Sep. 1970.

[16] Werlé, H., "Sur l'éclatement des tourbillons", ONERA Note Technique No. 175, Châtillon, France, Nov. 1971.

[17] Behrbohn, H., "Basic Low-Speed Aerodynamics of the Short-Coupled Canard Configuration of Small Aspect Ratio", SAAB, Sweden, TN-60, July 1965.

[18] Hummel, D., "Zur Umstronmung scharfkantiger schlanker Deltaflugel bei grossen Anstellwinkeln", Z. Flugwiss, Vol. 15, No. 10, 1967, pp. 376-385.

[19] Alexander, A.J., "Experiments on a Delta Wing Using Leading-Edge Blowing to Remove Secondary Separation", Aeronautical Research Council No. 24996, May 1963.

[20] Trebble, W.J.G., "Exploratory Investigation of the Effects of Blowing from the Leading-Edge of a Delta Wing", Aeronautical Research Council R&M No. 3518, 1966.

[21] Dixon, C.J., "Lift Augmentation by Lateral Blowing Over a Lifting Surface", AIAA-69-193, AIAA/AHS VTOL Research, Design, and Operations Meeting, Atlanta, Georgia, Feb. 1969.

[22] Cornish, J.J., III, "High Lift Applications of Spanwise Blowing", ICAS Paper No. 70-09, 7th Congress of the International Council of the Aeronautical Sciences, Rome, Italy, Sep. 1970.

[23] Smith, C.W., Ralston, J.N., Mann, H.W., "Aerodynamic Characteristics of Forebody and Nose Strakes Based on F-16 Wind Tunnel Test Experience, Vol. 1: Summary and Analysis", NASA CR-3053, July 1979.

[24] Rao, D.M., "Leading-edge Vortex Flap Experiments on a 74º Delta Wing", NASA CR 159161, 1979.

[25] Marchman, J.F. III, "Effectiveness of Leading-edge Vortex Flaps on 60 and 75 Degree Delta Wings", *Journal of Aircraft*, Vol.. 18, No. 4, 1981, pp. 280-286.

[26] Lamar, J.E., "Analysis and Design of Stake-Wing Configuration", *Journal of Aircraft*, Vol. 17, No. 1, 1980, pp. 20-27.

[27] Gursul, I., Yang, H., Deng, Q., “Control of Vortex Breakdown with Leading-Edge Devices”, AIAA-95-0676, 33rd AIAA Aerospace Sciences Meeting and Exhibit. Reno, NV, Jan. 1995.
[28] Gu, W., Robinson, O., Rockwell, D., “Control of Vortices on a Delta Wing by Leading-Edge Injection”, AIAA Journal, Vol. 31, No. 7, July 1993, pp.1177-1186.
[29] Bradley, R.G., Wray, W.O., "A Conceptual Study of Leading-Edge-Vortex Enhancement by Blowing", *Journal of Aircraft*, Vol. 11, No. 1, Jan. 1974, pp. 33-38.
[30] Guillot, S., Gutmark, E.J., Garrison, T.J., “Delay of Vortex Breakdown over a Delta Wing via Near-Core Blowing”, AIAA-98-0315, 35th AIAA Aerospace Sciences Meeting and Exhibit, Reno, NV, Jan. 1998.
[31] Mitchell, A.M., Molton, P., Barberis, D., Délery, J., “ Control of Vortex Breakdown Location by Symmetric and Asymmetric Blowing,” AIAA-99-3652, 30th AIAA Fluid Dynamics Conference, Norfolk, VA, June 1999.
[32] Mitchell, A.M., Molton, P., Barberis, D., Gobert, J.-L., “Control of Vortex Breakdown by Along the Core Blowing”, AIAA-00-2608, AIAA Fluids 2000 Conference, Denver, CO, June 2000.
[33] Kuo, C-H., Lu, N-Y., “Unsteady Vortex Structure over Delta Wing Subject to Transient Along-Core Blowing,” *AIAA Journal*, Vol. 36, No. 9, Sept 1998, pp. 1658-1664.
[34] Campbell, J.F., "Augmentation of Vortex Lift by Spanwise Blowing", *Journal of Aircraft*, Vol.13, No. 9, Sep.1976, pp.727-732.
[35] Anglin, E., Satran, D., "Effects of Spanwise Blowing on Two Fighter Configurations", AIAA-79-1663, AIAA Atmospheric Flight Mechanics Conference for Future Space Systems, Boulder, CO, Aug. 1979.
[36] Spillman, J. Goodridge, M., “Flow Characteristics About a Delta Wing at 15° Incidence with and without Edge Blowing”, Cranfield Report Aero. No. 9, April 1972.
[37] Shi, A., Wu, J.M., Vakili, A.D., “An Investigation of Leading-Edge Vortices on Delta Wings with Jet Blowing”, AIAA-87-0330, 25th AIAA Aerospace Sciences Meeting and Exhibit, Reno, NV, Jan. 1987.
[38] Visser, K.D., Iwanski, K.P., Nelson, R.C., Ng, T.T., “Control of Leading Edge Vortex Breakdown by Blowing”, AIAA-88-0504, 26th AIAA Aerospace Sciences Meeting and Exhibit, Reno, NV, Jan. 1988.
[39] Wood, N.J., Roberts, L., “Control of Vortical Lift on Delta Wings by Tangential Leading-Edge Blowing”, *Journal of Aircraft*, Vol. 25, No. 3, March 1988, pp. 236-243.
[40] Helin, H.E., "Effects of Trailing-Edge Jet Entrainment on Delta Wing Vortices", *AIAA Journal*, Vol. 32, No. 4, Apr. 1994, pp. 802-804.
[41] Shih, C., Ding, Z., “Trailing-Edge Jet Control of Leading Edge Vortices of a Delta Wing”, *AIAA Journal*, Vol. 34, No. 7, July 1996, pp. 1447-1456.
[42] Vorobieff, P.V. Rockwell, D.O., “Vortex Breakdown on Pitching Delta Wing: Control by Intermittent Trailing-Edge Blowing”, *AIAA Journal*, Vol. 36, No. 4, April 1998, pp.585-589.
[43] Mitchell, A.M., Molton, P., Barberis, D., Délery, J., “Control of Leading-Edge Vortex Breakdown by Trailing Edge Injection”, AIAA-99-3202, 17th AIAA Applied Aerodynamics Conference, Norfolk, VA, June-July 1999.
[44] Parmenter, K., Rockwell, D., "Transient Response of Leading-Edge Vortices to Localized Suction", *AIAA Journal*, Vol. 28, No. 6, 1990, pp. 1131-1132.
[45] Owens, D.B., Perkins, J., "Vortex Suppression on Highly-Swept Wings by Suction Boundary-Layer Control”, AIAA 95-0683, 33rd Aerospace Sciences Meeting and Exhibit, Reno, NV, Jan. 1995.
[46] Guy, Y., Morrow, J.A., McLaughlin, T.E., “Control of Vortex Breakdown on a Delta Wing by Periodic Blowing and Suction,” AIAA-99-0132, 37th AIAA Aerospace Sciences Meeting and Exhibit, Reno, NV, Jan. 1999.
[47] Guy, Y., Morrow, J.A., McLaughlin, T.E., Wygnanski, I., “Velocity Measurement on a Delta Wing with Periodic Blowing and Suction,” AIAA-2000-0550, 38th AIAA Aerospace Sciences Meeting and Exhibit, Reno, NV, Jan. 2000.
[48] Morton, S.A., Guy, Y., Morrow, J.A., Blake, D.C., “Numerical Simulation of Periodic Suction and Blowing Control of Vortex Breakdown on a Delta Wing,” AIAA-99-3195, 17th AIAA Applied Aerodynamics Conference, Norfolk, VA, June-July 1999.
[49] Guy, Y., Morton, S.A., Morrow, J.A., “Numerical Investigation of the Flow Field on a Delta Wing with Periodic Blowing and Suction,” AIAA-2000-2321, Fluids 2000, Denver, CO, June 2000.
[50] Afchain, D., Broussaud, P., Frugier, M., Rancarani, G., "La soufflerie F2 du centre du Fauga-Mauzac," ONERA TP 1983-139, No. 193880, 1983.
[51] Pagan, D., Molton, P. Solignac, J.L., "Etude expérimentale et simulation numérique de l’éclatement d’un tourbillon d’ailettes", ONERA Rapport Technique n 38/1147 AY, Sep. 1988.
[52] Laval-Jeantet, R., "Contribution à l'étude du contrôle actif de l'éclatement tourbillonnaire sur aile en flèche en écoulement incompressible," Thesis de doctorant, Université d'Aix-Marseille II, Marseille, Mar. 1993.
[53] Barberis, D., "Test Cases for CFD Validation," Onera TP No. 1993-161, Châtillon, France, 1993.
[54] Guy, Y., Morrow, J. A., McLaughlin, T. A. and Wygnanski, I., “Pressure Measurement and Flow Field Visualization on a Delta Wing with Periodic Blowing and Suction”, AIAA Paper 99-4178, August 1999.
[55] Guy, Y., Morrow, J. A., McLaughlin, T. A. and Wygnanski, I., “Parametric Investigation of the Effects of Active Control on the Normal Force on a Delta Wing”, AIAA Paper 2000-0549, January 2000.
[56] Strang, W. Z., Tomaro, R. F., Grismer, M. J., “The Defining Methods of Cobalt: A Parallel, Implicit, Unstructured Euler/Navier-Stokes Flow Solver,” AIAA 99-0786, January 1999.
[57] Samareh, J., “Gridtool: A Surface Modeling and Grid Generation Tool,” Proceedings of the Workshop on Surface Modeling, Grid Generation, and Related Issues in CFD Solution, NASA CP-3291, May 9-11, 1995.
[58] Pirzadeh, S., “Progress Toward A User-Oriented Unstructured Viscous Grid Generator,” AIAA Paper 96-0031, January 1996.
[59] Visbal, M. R: “Computational and Physical Aspects of Vortex Breakdown on Delta Wings”, AIAA Paper 95-0585, January 1995.

[60] Iwanski, K. P., Ng, T. T. and Nelson, R. C., “An Investigation of the Vortex Flow over a Delta Wing with and without External Jet Blowing”, Master Thesis, University of Notre Dame, Indiana, 1988.

[61] Agrawal, S. A. and Barnett, R., “Numerical Investigation of Vortex Breakdown on a Delta Wing”, AIAA Journal, Vol. 30, No. 3, pp 584-591, March 1992.